Cellular Signalling 26 (2014) 352–362

Contents lists available at ScienceDirect

Cellular Signalling

journal homepage: www.elsevier.com/locate/cellsig

Dorsomorphin reverses the mesenchymal phenotype of breast cancer initiating cells by inhibition of bone morphogenetic protein signaling

Chiara Garulli [1], Cristina Kalogris [1], Lucia Pietrella, Caterina Bartolacci, Cristina Andreani, Maurizio Falconi, Cristina Marchini *, Augusto Amici *

Department of Bioscience and Biotechnology, University of Camerino, Camerino 62032, Italy

ARTICLE INFO

Article history:
Received 5 June 2013
Received in revised form 12 November 2013
Accepted 19 November 2013
Available online 23 November 2013

Keywords:
Bone morphogenic proteins
Mesenchymal cancer stem cells
Breast cancer
Dorsomorphin
EMT (epithelial–mesenchymal transition)

ABSTRACT

Increasing evidence supports the theory that tumor growth, homeostasis, and recurrence are dependent on a small subset of cells with stem cell properties, redefined cancer initiating cells (CICs) or cancer stem cells. Bone morphogenetic proteins (BMPs) are involved in cell-fate specification during embryogenesis, in the maintenance of developmental potency in adult stem cells and may contribute to sustain CIC populations in breast carcinoma. Using the mouse A17 cell model previously related to mesenchymal cancer stem cells and displaying properties of CICs, we investigated the role of BMPs in the control of breast cancer cell plasticity. We showed that an autocrine activation of BMP signaling is crucial for the maintenance of mesenchymal stem cell phenotype and tumorigenic potential of A17 cells. Pharmacological inhibition of BMP signaling cascade by Dorsomorphin resulted in the acquisition of epithelial-like traits by A17 cells, including expression of Citokeratin-18 and E-cadherin, through downregulation of Snail and Slug transcriptional factors and Cyclooxygenase-2 (COX2) expression, and in the loss of their stem-features and self-renewal ability. This phenotypic switch compromised A17 cell motility, invasiveness and *in vitro* tumor growth. These results reveal that BMPs are key molecules at the crossroad between stemness and cancer.

1. Introduction

BMPs are extracellular signaling molecules belonging to the transforming growth factor-β (TGF-β) family, which includes 33 members in mammals. These factors control various cellular processes, such as proliferation, differentiation, apoptosis and migration. They exert their functions by binding to two distinct transmembrane serine–threonine kinase receptors, type I and type II, and forming a heterotetrameric complex [1]. Three BMP type I receptors (BMPRIA/ALK-3, BMPRIB/ALK-6, BMPR2) and three BMP type II receptors (ACVR1, ACVR2, ACVR2B) have been characterized. In the complex, type II receptor phosphorylates and activates the type I receptor that in turn can transmit the signal through SMAD dependent and SMAD independent pathways, including ERK, JNK, and p38 MAP kinase pathways [2,3]. SMAD signaling involves phosphorylation and activation of receptor-activated SMADs (R-SMADs), which in turn form complexes with the common partner SMAD4 (Co-SMADs) [3,4]. The R-SMAD/Co-SMAD complexes then translocate into the nucleus and regulate transcription of target genes by interacting with various transcription factors and transcriptional co-activators or co-repressors. Among the eight SMAD proteins identified in mammals, SMAD1, SMAD5, and SMAD8 are activated by BMP type I receptors, whereas SMAD2 and SMAD3 are activated by activin and TGF-β type I receptors. SMAD4 is the only Co-SMAD in mammals, which is shared by both BMP and TGF-β/activin signaling pathways [4]. Although aberrant expression of BMPs has been reported in several cancers, the role of BMP signaling in breast cancer initiation and progression remains unclear. Many studies have reported contradicting results, with some investigators finding that BMP signaling promotes tumor growth and others reporting tumor suppressive effects [5,6]. Given the demonstrated impact of BMPs in various stem cell populations [7,8], these molecules may contribute to the maintenance of CIC population in breast carcinoma. The interwoven nature of pluripotency and tumorigenicity programs is revealed by the molecular machinery shared by them, and it has become a major challenge to untangle the determinants of pluripotency from those responsible for tumorigenicity. A17 cells are a highly tumorigenic and invasive mesenchymal cell line, established from a FVB/neuT transgenic mammary tumor, displaying properties of CICs. We previously showed that A17 cells exhibit a stemness-related gene signature which was virtually identical to that of mesenchymal stem cells and are endowed with the self renewal ability [9]. Comparative gene expression profiling of A17 cells and mesenchymal stem cells revealed that only very few

* Corresponding authors. Tel.: +39 0737 403275.
E-mail addresses: cristina.marchini@unicam.it (C. Marchini), augusto.amici@unicam.it (A. Amici).
[1] These authors contributed equally to this work.

0898-6568/$ – see front matter © 2013 Elsevier Inc. All rights reserved.
http://dx.doi.org/10.1016/j.cellsig.2013.11.022

genes were differentially expressed. Among them, bone morphogenetic protein-4 (BMP4) displayed a two-fold higher expression in A17 cells than in mesenchymal stem cells, suggesting a special role for this molecule in A17 tumorigenicity [9]. Moreover, A17 cells significantly overexpress COX2, a mesenchymal hallmark in tumors, whose relevance in growth, vasculogenesis and invasiveness has been widely documented in various types of carcinoma, both in clinical and experimental studies [10,11]. Taken together, the characteristics of A17 cells make them an attractive model of CICs. Herein, we investigated the role of BMP signaling cascade in the maintenance of mesenchymal stem cell phenotype and tumorigenic potential in A17 cells identifying a new BMP4/COX2 axis as a crucial pathway in the control of breast tumor plasticity.

2. Materials and methods

2.1. Cell cultures

A17 and BB1 cell lines were established from spontaneous HER-2/neu transgenic tumors as previously described [12,13] and were cultured in Dulbecco's Modified Eagle Medium (DMEM, Invitrogen) supplemented with 20% fetal bovine serum (FBS, Invitrogen) and 100 U/ml penicillin–100 μg/ml streptomycin (Invitrogen). Dorsomorphin (Sigma-Aldrich) was dissolved in Dimethyl sulfoxide (DMSO, Sigma-Aldrich) and directly added to the medium at a final concentration of 0.5 μM and 2 μM. Medium was changed daily for four days. Cells were treated in the same way with prostaglandin E (2) (PGE_2, Sigma Aldrich) at 5 μM and BMP4 (R&D System) at 20 ng/ml final concentration. Cells treated with media containing an equivalent amount of DMSO of the maximal inhibitor concentration served as a negative control. DMSO-treated cells had similar outcomes to control untreated cells, indicating that DMSO had no effect on A17 cell growth.

siRNA knockdown experiments were performed by transient transfection of A17 cells with 50 nM of a pool of four different siRNA molecules (Riboxx), targeting BMP4 or TGF-β type I receptor or non-targeting scramble as control (Supplementary Table 1). Interferin (Polyplus-transfection) was used as siRNA transfection reagent following the manufacturer's instructions. Effects of BMP4 or TGF-β type I receptor silencing on the morphology of A17 cells and on their expression of epithelial–mesenchymal transition (EMT) markers were evaluated 72 h and 96 h after transfection.

2.2. RNA, RT-PCR, quantitative PCR

Total RNA was extracted using the NucleoSpin RNAII kit (Macherey-Nagel) according to manufacturer's instructions. 1 μg of total RNA was reverse-transcribed using the RevertAID H Minus First Strand cDNA Synthesis Kit (Fermentas). The cDNA templates were then analyzed by RT-PCR with standard protocol. Amplicons were analyzed on agarose gel electrophoresis.

Quantitative PCR was performed on a Real Time PCR System (Stratagene, Mx3000P) using the real master mix kit (Eppendorf, Milano, Italy), containing SYBR Green (1 mM dNTPs, 10 mM $(CH_3COO)2$ Mg and 0.05 U/μl HotMaster Taq polymerase). Primer sequences used are reported in Table 1.

2.3. Immunoblotting analysis

Cells were lysated directly into the 25 cm^2 culture flasks using a boiling sample buffer without beta-mercaptoethanol (50 mM Tris pH 6.8, 2% SDS, 10% Glycerol). Lysates were separated by 4–20% gradient precast SDS-PAGE (Bio-Rad) and transferred onto polyvinylidene difluoride (PVDF) membranes (Immobilon P, Millipore, Milano, Italy). Antibodies to Cyclin D1, Snail, Slug, Src, pTyr416 Src, p38, pP38, SMAD1, pSMAD1/5/8, pSMAD2 and Alk3, AcvR2, BMPRII, ID1, Vimentin were from Cell Signaling (Beverly, MA, USA). Antibody to COX2 was from Cayman Chemical (Ann Arbor, MI, USA). Antibodies to SCA-1 and Notch-1 were from BD Transduction Laboratories (Franklin Lakes, NY, USA). Antibody to Cytokeratin 18 was from Epitomics (Burlingame, CA, USA). Secondary antibodies conjugated with peroxidase were from Sigma-Aldrich (St. Louis, MO, USA). The immunoreactive bands were detected with ECL detecting reagents (Amersham Bioscience, Little Chalfont, UK).

Table 1
Primer sequences.

Genes	Primer sequences
ID1 forward	5′-GCACTGAGGGACCAGATGG-3′
ID1 reverse	5′-GGCTCTGTTGATCAAACCC-3′
COX2 forward	5′-TGCTCACGAAGGAACTCAGC-3′
COX2 reverse	5′-CTCATACATTCCCCACGGTTTTG-3′
E-Cadherin forward	5′-TTCCAGGAACCTCCGTGATG-3′
E-Cadherin reverse	5′-CAGGCACTTGACCCTGATAC-3′
BMP4 forward	5′-GTACCCGGAGCGTCCCGC-3′
BMP4 reverse	5′-GGGCCCTGGTCCACCTGC-3′
ALK3 forward	5′-GACTTCCTGAAATGTGC-3′
ALK3 reverse	5′-CGATGAGCAATTGCAGGC-3′
GADPH forward	5′-GACAAAATGGTGAAGGTCGG-3′
GADPH reverse	5′-TCAGCACCGGCCTCACCC-3′
GADPH 2 forward	5′-GAAGCTTGTCATCAACGGGAAG-3′
GADPH 2 reverse	5′-ACTCCACGACATACTCAGCAC-3′

2.4. Flow cytometry

Cells were dissociated into single cell suspension and 1×10^6 cells were used per sample. For membrane antigens cells were washed in staining buffer (0.1% NaN_3, 2% FBS in PBS), incubated with the primary antibody 1 h at 4 °C and then after three washes they were incubated with labeled secondary antibody 1 h at 4 °C. Washed cells were resuspended in PBS and assessed by FACS equipped with Cell Quest software (BD Pharmingen), data analysis was performed using FlowJo software. To label internal antigens BD fix and BD perm solutions were used according to manufacturer's instructions.

2.5. Cell viability assay

Dorsomorphin effect on A17 cells was evaluated by seeding 5×10^6 cells in 96 well plates in complete medium (DMEM supplemented with 20% of FBS). The day after fresh medium containing appropriate Dorsomorphin concentrations was added. Cell viability was determined using an MTT [3-(4,5-dimethylthiazol-2-yl)-2,5-diphenyl-2H-tetrazolium bromide Sigma Aldrich] assay after 96 h. Each drug concentration was evaluated with 16 replicates and the experiment was repeated three times.

2.6. Flow cytometry analysis of cell cycle and apoptosis

Cell-cycle status and apoptosis analysis were performed using flow cytometry. Briefly, cells were plated at a density of 1×10^5 cells/well in 6 well plates and maintained in medium containing 20% FBS overnight. The following day, cells were treated with 0.5 or 2 μM Dorsomorphin in medium containing 20% FBS for the indicated length of time. Cells were harvested, labeled and assessed by FACS equipped with Cell Quest software (BD Pharmingen), data analysis was performed using FlowJo software. Apoptosis of cells was evaluated by measuring the exposure of phosphatidylserine on the cell membranes using an Apoptosis Detection Kit (BD Pharmingen). Cells were labeled in a staining solution containing 50 μg/ml PI and 25 μg/ml Annexin V-FITC for 15 min at room temperature in the dark, according to manufacturer's instructions. For DNA analysis, cells were fixed with ice-cold 70% ethanol, RNA was degraded using 1 mg/ml bovine RNase (Sigma Aldrich) and then labeled

with a solution containing 15 μg/ml PI (propidium iodide). After 30 min, DNA content was analyzed using flow cytometry. Both the experiments were repeated three times.

2.7. Cell invasion and migration

Cell invasion and migration assays were carried out using modified Boyden chambers consisting of transwell (BD Biosciences, 6.5 mm diameter, 8 μm pore size, 10 mm thickness polycarbonate membranes) membrane filter inserts in 24 well tissue culture plates. The bottom surfaces of the transwell membranes were coated with fibronectin (10 μg/ml) in both the assays, for invasion assay also upper surfaces were coated with 1 mg/ml Matrigel matrix (BD Biosciences) diluted in DMEM (1/3). After 24 h in starvation, 8×10^3 A17 cells were seeded in DMEM with 2%BSA (Sigma Aldrich) on the upper transwell surfaces and allowed to invade toward the underside of the membrane for 16 h. Non-invading cells were removed by wiping the upper side of the membrane, and the migrating/invading cells were fixed and stained using Diff-Quik (Baxter Healthcare Corp., McGraw Park, IL). Cells were counted under a microscope in eight randomly chosen fields.

2.8. Wounding assay

A17 cells were seeded into six well plates and when they reached confluence the experiment was carried out. The cell monolayer was scratched in the middle with a plastic tip and then treated with Dorsomorphin. To prevent proliferation during wounding assay, cells were starved. Migration was monitored by optical inspection for 16 h using an Olympus microscope (Olympus, Hamburg, Germany) and pictures were taken at 0 and 16 h. This experiment was repeated three times.

2.9. Soft agar assay

Anchorage-independent cell proliferation was determined by a soft agar assay, using a modification of previously described methods [14]. Briefly, a base layer of 0.5% agar in complete medium was plated in six-well plates and allowed to solidify (Dorsomorphin and BMP4 synthetic protein were added into appropriate wells). Next, triplicate wells were overlaid with 6×10^7 cells per well in a 0.35% agar. The plates were incubated at 37 °C, 5% CO_2 for 15 days. Dishes were stained with 0.05% crystal violet overnight at 4 °C. Colonies were counted in ten randomly chosen fields.

2.10. Mammosphere cultures

For generation of mammospheres, A17 cells were first grown in six well low-attachment plates (Costar) at 1×10^5 cells per well [15]. Suspension cultures were incubated for 15 days to obtain colonies. Colonies were then enzymatically dissociated with 0.05% trypsin and 0.53 mM EDTA (Invitrogen) and seeded at the dilution of one half cell per well into 96 well low-attachment plates in serum-free DMEM media supplemented with B27 (Invitrogen, Carlsbad, CA), 20 ng/ml EGF (Sigma, St. Louis, MO), 20 ng/ml bFGF (Sigma), and 4 μg/ml heparin (Sigma). After 15 days, the first generation of mammospheres was obtained. The efficiency of mammosphere formation by single cells was monitored microscopically.

2.11. Capillary-like tubule formation assay

The Matrigel basement membrane matrix (BD Biosciences) was used to assess tubular structure formation according with previously described methods [16]. Matrigel was thawed overnight at 4 °C and diluted 1/3 in DMEM. Next day, 50 μl of Matrigel dilution was added to each well of a 96-well plate. The Matrigel matrix was allowed to polymerize at room temperature for 20 min. 5×10^3 cells were seeded on the Matrigel top. All assays were performed in triplicate. Cells were incubated for 48 h at 37 °C and then observed using an IX70 Olympus microscope.

2.12. Luciferase assay

COX2 promoter luciferase reporter plasmids were generated as previously described [17]. A17 cells were seeded in 24 well plates (8×10^4 cells/well), then they were transiently transfected with COX2-promoter luciferase reporter plasmids with Lipofectamine 2000 (Invitrogen) in Optimem. After 16 h, Optimem was substituted with DMEM supplemented with 2% FBS and Dorsomorphin or BMP4. After incubation for a further 24 h, luciferase assays were performed on cell lysates using the luciferase assay system (Promega) in a Berthold LB-953 luminometer. pGL3-control vector (Promega), in which the luciferase expression is driven by SV40 promoter, was used as positive control, while a pGL3 without the promoter sequence was used as negative control. Luciferase activity was expressed as relative light units per mg of cell proteins as determined by Bio-Rad Protein Assay Dye Reagent (Bio-Rad). Each experiment was prepared in triplicate, and repeated two times.

2.13. Statistical analysis

Statistical analysis was performed using student's *t* test or one-way ANOVA followed by Bonferroni's multiple comparison tests. Quantitative data are presented as means ± SEM. Differences were considered significant at $^*P \leq 0.05$; $^{**}P \leq 0.01$; $^{***}P \leq 0.001$.

3. Results

3.1. BMP4 controls A17 cell signaling through an autocrine positive feedback

Comparative analysis of A17 cells and mesenchymal stem cells, revealed that BMP signaling pathway components are expressed in both cell models [9]. Since BMP4 was differentially expressed between the two cell lines, being expressed two-fold higher in A17 cells than in mesenchymal stem cells, we focused on the pathway activated by this molecule. First, we verified the expression of BMP receptors ALK3, BMPRII and Acvr2 on A17 cell surface by FACS analysis (Fig. 1A). Then, we analyzed the activation of the intracellular signaling pathways downstream the receptors. One of the best characterized signal transduction pathways that mediates the actions of BMP4 is that leading to the phosphorylation of SMAD1/5/8. However BMPs can also activate p38 through the SMAD-independent pathway. Accordingly, we examined the phosphorylation of both SMAD1/5/8 and p38 by Western blotting using specific anti-phospho-SMAD1/5/8 and anti-phospho-p38 antibodies. The obtained results, showing phosphorylation of both SMAD1/5/8 and p38, proved the intracellular transduction of BMP signal (Fig. 1B). This finding was confirmed also by the massive expression of ID1, which is a known BMP target gene [1,18,19] (Fig. 1A). Phosphorylation of SMAD2 demonstrated signaling transduction even by TGF-β. The presence of phosphorylated forms of SRC and STAT3 indicated the activation of further alternative pathways (Fig. 1B).

To dissect the signaling pathways downstream BMPs, we used Dorsomorphin, a selective small molecule inhibitor of BMP type I receptors which inhibits BMP signaling in preference to TGF-β, activin, and other ligands of the TGF-β family [20,21]. The ability of Dorsomorphin to functionally separate BMP-mediated activation of SMAD1/5/8 was verified by Western blotting analysis. Dorsomorphin drastically reduced phosphorylation of SMAD1/5/8 in a dose-dependent manner, but had much less effect on the activation of p38 and did not alter TGF-β specific SMAD2 phosphorylation. STAT3 phosphorylation state remained also totally unchanged after Dorsomorphin treatment, while SRC activation was only slightly affected (Fig. 1B). The selective interference of

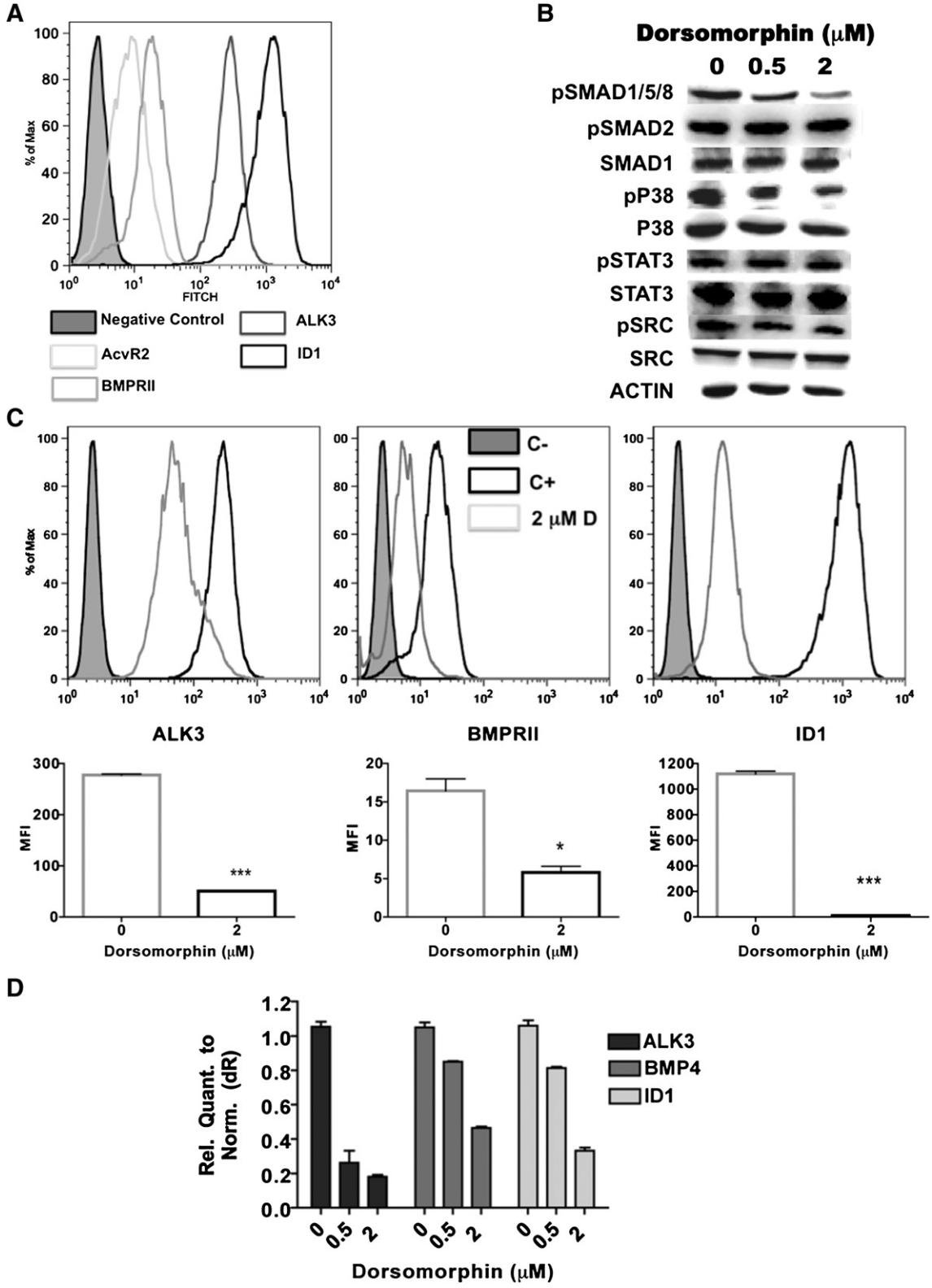

Fig. 1. BMP signaling pathway in A17 cells. (A) Flow cytometry histograms of BMP type I receptors ALK3 (BMPRIA) and BMPRII, BMP type II receptor AcvR2, and BMP target gene ID1. (B) Western blot analysis of BMPs downstream signaling pathways in control (vehicle alone) and Dorsomorphin treated A17 cells. Cell extracts were probed with antibodies to pSMAD1/5/8, pSMAD2, SMAD1, pp38, p38, pSTAT3, STAT3, pSRC and SRC. Actin was used as loading control. (C) Flow cytometry histograms of BMP receptors (ALK3 (BMPRIA) and BMPRII) and the target gene ID1 in control (vehicle alone) and Dorsomorphin treated A17 cells. Results were shown also as MFI (mean fluorescence intensity). (D) ALK3, BMP4 and ID1 mRNAs were measured by quantitative RT-PCR in control (vehicle alone) and Dorsomorphin (0.5 μM or 2 μM) treated A17 cells, normalized to glyceraldehyde-3-phosphate dehydrogenase (GAPDH) and shown as mean ± SEM of three independent experiments. *$P \leq 0.01$; ***$P \leq 0.001$, One way ANOVA followed by Bonferroni's multiple comparison test.

Dorsomorphin with SMAD1/5/8 mediated signaling pathway led to a strong reduction of both ID1 protein and RNA expression (Fig. 1C, D). Interestingly, Dorsomorphin significantly decreased in a dose dependent manner the mRNA levels of BMP4 and the expression of its receptors, ALK3 and BMPRII, as shown by FACS analysis and semi-quantitative RT-PCR (Fig. 1C, D).

All together, these results confirmed the expression of BMPs by A17 cells, as well as the presence of the type I and type II BMP receptors and SMADs required for BMP signal transduction. Moreover these findings provide evidences for a crucial role of BMP4 in the control of A17 cell signaling through an autocrine positive feedback.

3.2. BMP pathway is required to maintain mesenchymal phenotype

To investigate the role of BMPs in the control of CIC phenotype, we treated A17 cells with Dorsomorphin. Remarkably, upon four days of Dorsomorphin treatment, A17 cells underwent a switch from an elongated mesenchymal phenotype to a polygonal epithelial-like shape, evident in both confluent and sub-confluent culture conditions (Fig. 2A). This morphological transition correlated with a dose-dependent decrease in the expression of Vimentin, a typical mesenchymal marker, and with a drastical reduction of the transcriptional factors Snail and Slug, known to repress E-cadherin expression during EMT (Fig. 2B) [22,23]. Consistently, quantitative Real Time PCR experiments and Western blot analysis showed that E-cadherin was induced in a dose-dependent manner upon Dorsomorphin treatment, both at mRNA and protein levels (Fig. 2C, B). Moreover, BMP pathway inhibition induced a strong expression of Cytokeratin-18, another epithelial marker (Fig. 2B). Similar results were obtained by transfection of A17 cells with siRNA molecules targeting BMP4. In fact, BMP4 siRNA suppressed Vimentin expression and induced instead Cytokeratin-18, thereby shifting cellular morphology toward an epithelial phenotype, while A17 cells treated with siRNA targeting type I TGF-β receptor or scramble siRNA maintained their spindle shape In addition, RT-PCR and quantitative RT-PCR analyses confirmed that suppression of BMP4 by siRNA is concomitant with the induction of the expression of E-cadherin mRNA in A17 cells (Supplementary Fig. 1).

These experiments revealed the pivot role of BMP autocrine signaling in the maintenance of the mesenchymal stem cell phenotype, identifying potential target molecules for therapies aimed to reduce recurrence risk.

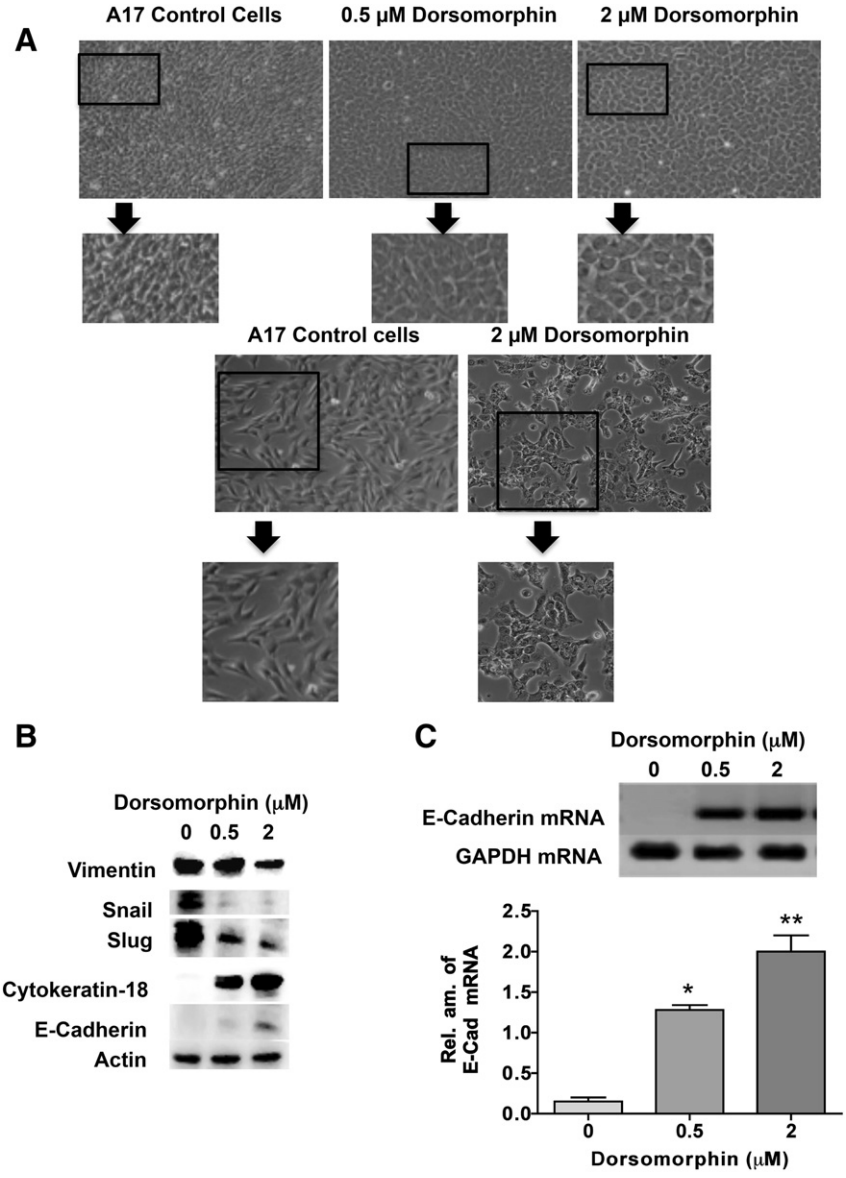

Fig. 2. Dorsomorphin promotes mesenchymal to epithelial transition (MET) in A17 cells. (A) Representative images of control (vehicle alone) and Dorsomorphin treated A17 cells. Cells were visualized by phase-contrast microscopy. Magnification ×10. Insert magnification ×20. (B) Western blot analysis of Vimentin, Snail, Slug, Cytokeratin 18 and E-cadherin levels indicates that treatment of A17 cells with Dorsomorphin causes changes that are consistent with MET. Actin was used as loading control. (C) RT-PCR and quantitative RT-PCR analyses indicate that Dorsomorphin treatment induces the expression of E-cadherin mRNA in A17 cells. Expression levels are normalized to GAPDH. *P ≤ 0.05; **P ≤ 0.01 One way ANOVA followed by Bonferroni's multiple comparison test.

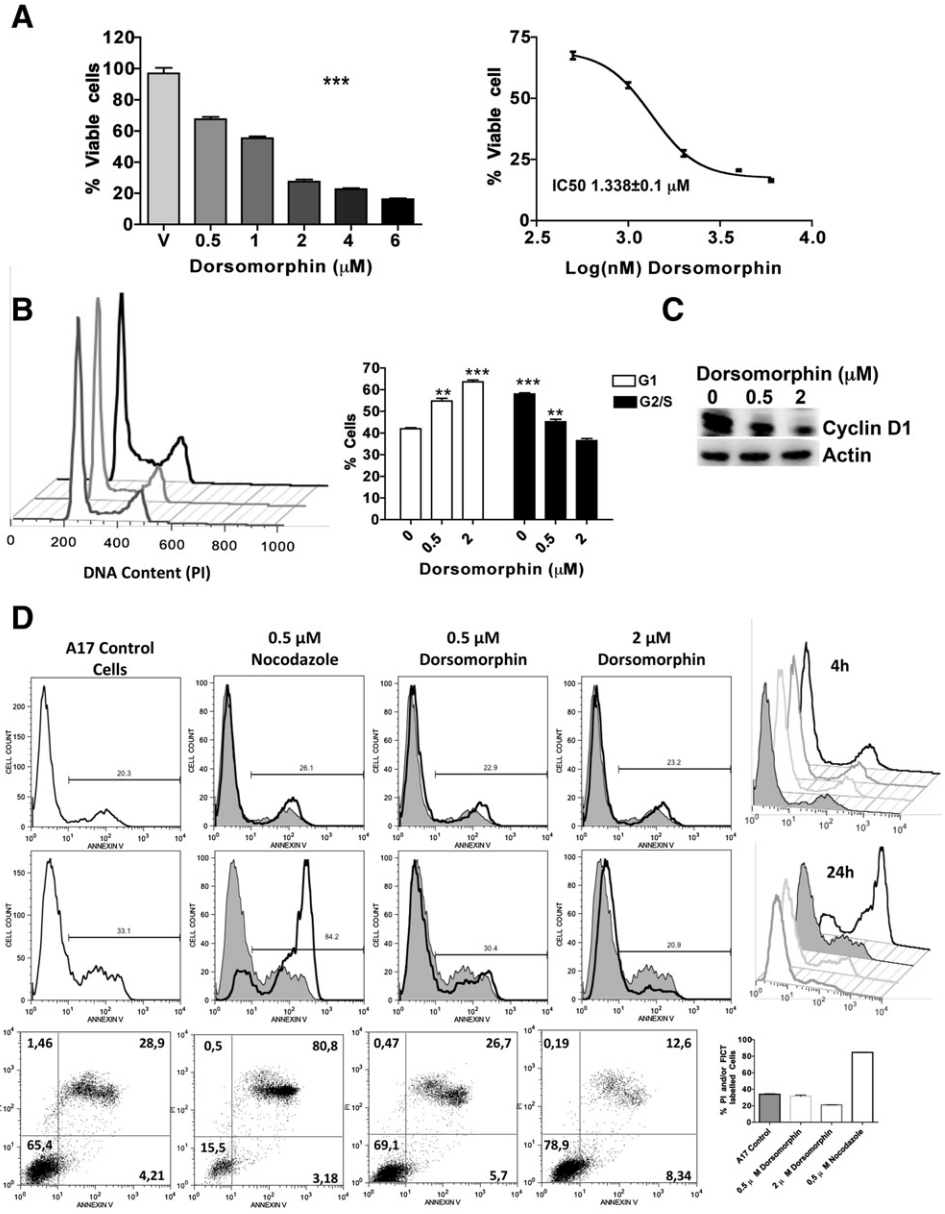

Fig. 3. Dorsomorphin has cytostatic effect in A17 cells. (A) A17 cells were incubated for 96 h in the presence of vehicle or increasing concentrations of Dorsomorphin and cell viability was assayed by 3-[4,5-dimethylthiazolyl-2] 2,5-diphenyl-tetrazolium bromide (MTT). The results are expressed as percentage of living cells in respect to control (vehicle alone) and are presented as mean ± SD ($n = 16$). IC50 of Dorsomorphin after 96 h was calculated to be 1.338 ± 0.1 μM. (B) Cell cycle analysis by flow cytometry of A17 cells treated with vehicle alone or Dorsomorphin (0.5 μM or 2 μM) for 48 h (left panel). Histogram plots summarizing FACS analysis. Data represent mean ± SEM of triplicate experiments (central panel). (C) Western blot analysis of cyclin D1 expression in control (vehicle alone) and Dorsomorphin (0.5 μM or 2 μM) treated A17 cells (right panel). (D) Quantification of apoptosis through Annexin V staining and FACS analysis. FACS histograms of A17 cells treated as indicated for 4 h (top panel) or for 24 h (central panel). Dual parameter dot plot of FITC-fluorescence (x-axis) vs propidium iodide (PI)-fluorescence (y-axis) has been shown (bottom panel). Histogram plots summarizing Annexin V staining and FACS analysis. Data represent mean ± SEM of triplicate experiments. **P ≤ 0.01; ***P ≤ 0.001, between treated samples and control. One way ANOVA followed by Bonferroni's multiple comparison test.

3.3. Cytostatic inhibition of A17 cells by Dorsomorphin

To evaluate the effect of BMP pathway on cell proliferation, we first performed an MTT assay on A17 cells treated with increasing doses of Dorsomorphin for 96 h. As shown in Fig. 3A, Dorsomorphin reduced viable cells in a dose-dependent manner and with an IC_{50} equal to 1.338 ± 0.1 μM. Flow cytometric analysis of cell cycle revealed that this decrease in cell population is due to a reduction in dividing cells (Fig. 3B). In fact, 20% of A17 cells treated with 2 μM Dorsomorphin for two days remained blocked at G1 phase instead to proceed into G2/S phase. This behavior correlated with a decreased expression of cyclin D1 (Fig. 3C). Analysis of apoptosis by flow cytometry revealed that Dorsomorphin did not cause apoptosis or necrosis (Fig. 3D). Indeed, the percentage of cells labeled with Propidium and Annexin V was not significantly different in treated and untreated cells even after 24 h incubation with 2 μM Dorsomorphin (Fig. 3D). Thus, BMP signaling pathway controls cell proliferation and tumorigenic potential of A17 cells.

3.4. BMP activated SMAD signaling strongly promotes migration, invasion and tumorigenicity of A17 cells

To assess the BMP contribution to breast cancer cell malignancy, the role of BMP pathway on migration, invasion and anchorage-independent growth was evaluated in A17 cells. As shown in Fig. 4, 2 μM Dorsomorphin treatment of A17 cells led to a 70% reduction in their ability to migrate as well as a 90% reduction in their ability to invade Matrigel. On the contrary, BMP4, acting as chemoattractant, enhanced motility and invasivity of A17 cells, confirming the crucial

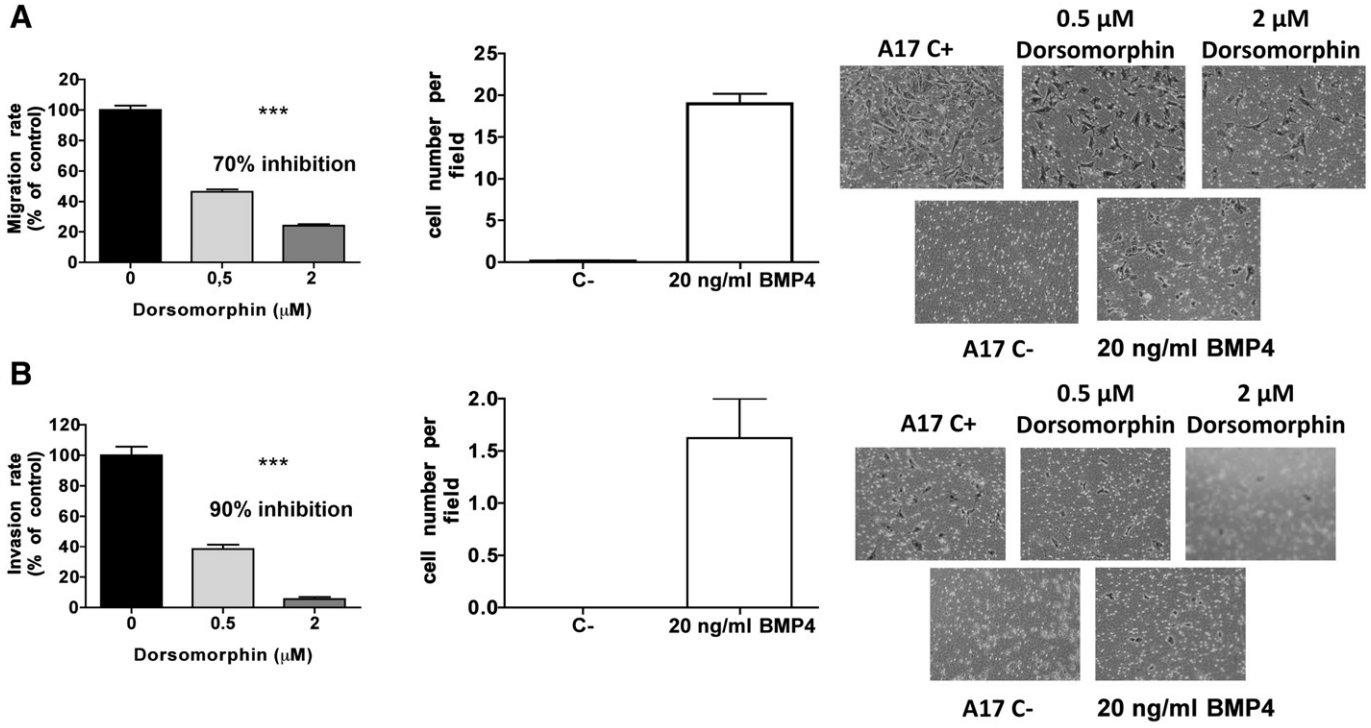
A
Migration rate (% of control)
***
70% inhibition
Dorsomorphin (μM)
cell number per field
C-
20 ng/ml BMP4
A17 C+
0.5 μM Dorsomorphin
2 μM Dorsomorphin
A17 C-
20 ng/ml BMP4
B
Invasion rate (% of control)
***
90% inhibition
Dorsomorphin (μM)
cell number per field
C-
20 ng/ml BMP4
A17 C+
0.5 μM Dorsomorphin
2 μM Dorsomorphin
A17 C-
20 ng/ml BMP4

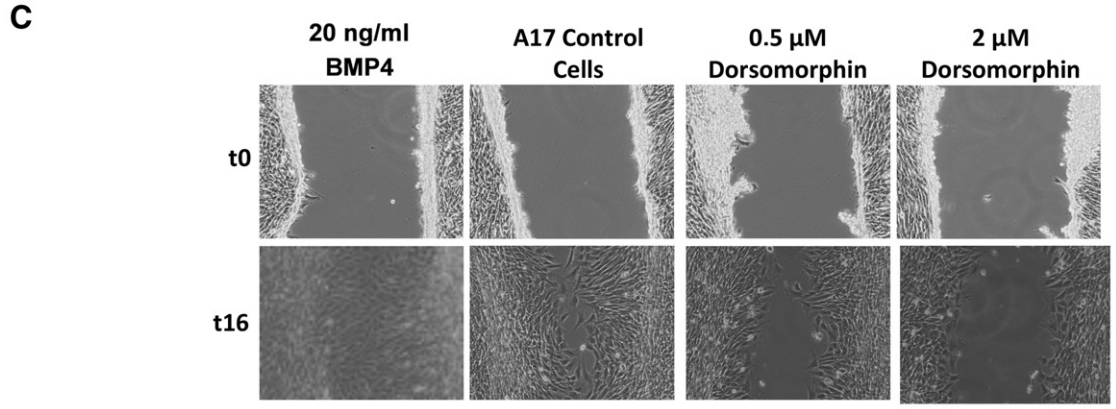
C
20 ng/ml BMP4
A17 Control Cells
0.5 μM Dorsomorphin
2 μM Dorsomorphin
t0
t16

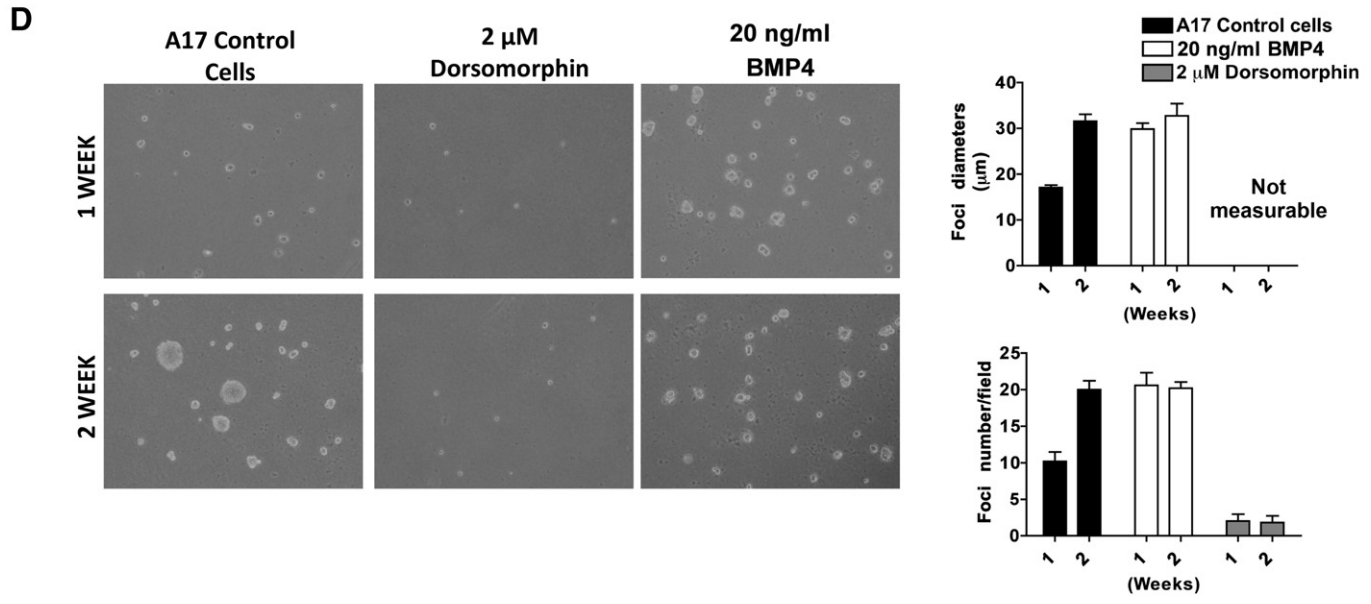
D
A17 Control Cells
2 μM Dorsomorphin
20 ng/ml BMP4
1 WEEK
2 WEEK
A17 Control cells
20 ng/ml BMP4
2 μM Dorsomorphin
Foci diameters (μm)
Not measurable
(Weeks)
Foci number/field
(Weeks)

role of this factor in the control of cancer stem cell functional properties (Fig. 4A, B). These data were supported by a wound-healing assay showing the ability of A17 cells to move and close the gap within 16 h. Treatment of A17 cells with BMP4 made even faster the wound closure, whereas Dorsomorphin blocked the cells at the edges of the wound (Fig. 4C). Consistently, BMP4 gene silencing retards A17 cell motility, while cell motility of A17 cells transfected with siRNA targeting type I TGF-β receptor was the same as that for cells transfected with the control siRNA (Supplementary Fig. 2).

As anchorage-independent growth is considered to be *in vitro* test for tumorigenesis, we examined the growth of A17 cells in a semi-soft agarose medium for two weeks. Scoring of the number and the size of the formed colonies revealed that BMP4 accelerated the formation of foci, although at the end of the experiment the colony number was comparable to control. On the contrary, Dorsomorphin drastically reduced the number and the size of foci (Fig. 4D).

3.5. BMP pathway promotes mammosphere formation by A17 cells

We have studied the role of BMP signaling in A17 mammosphere formation using Dorsomorphin. Formation of nonadherent spherical clusters of cells or mammospheres in low-attachment conditions is a characteristic of stem cells and cancer stem cells [24]. We found that A17 cells had a high capacity to grow in mammospheres, with approximately one in two cells capable of forming these structures until the fourth generation. This capability decreases in next generations (data not shown). 2 μM Dorsomorphin treatment had a dramatic effect on A17 self-renewal decreasing the number and the size of primary mammospheres (Fig. 5A). Accordingly, the expression of SCA-1 and Notch-1 stem markers were markedly reduced in Dorsomorphin treated cells (Fig. 5B). On the other hand, under BMP4 stimulation the number and the size of primary mammospheres significantly increased.

A Matrigel-based three-dimensional (3D) culture system was used to investigate the influence of BMP signaling on the morphogenetic properties of A17 cells in a closely resembling *in vivo* situation. Breast epithelial cells and mesenchymal stem cells develop into polarized and highly organized acinar and ductal structures in response to stromal cues, including extracellular matrix composition and density, which can in part be reproduced in 3D culture conditions. A17 cells formed tubular structures in Matrigel containing b-FGF, however upon Dorsomorphin treatment they formed well-differentiated round spheroids similar to those organized by BB1 breast cancer epithelial cells [12,13] (Fig. 5C).

These data suggested that BMP pathway is essential for maintenance of cancer stem-like cells in breast cancer.

3.6. BMP-dependent COX2 expression is involved in maintenance of mesenchymal phenotype

COX2 is frequently associated to aggressive breast cancer [11] and it was found significantly over-expressed in A17 cells, where it correlates with their mesenchymal signature [9,10,17]. Other studies have demonstrated the interaction between BMPs and COX2 [25]. Interestingly, treating A17 cells with Dorsomorphin the expression of COX2 markedly decreased in a dose dependent manner, both at protein and mRNA levels (Fig. 6A). In particular, COX2 mRNA almost disappeared as a consequence of the treatment with 2 μM Dorsomorphin, suggesting that BMPs exert a transcriptional control on COX2 expression. Accordingly, luciferase assays on two DNA fragments corresponding to a short (−965, +39) and a long (−3195, +39) COX2 promoter indicated that Dorsomorphin significantly decreased COX2 promoter activity, while BMP4 synthetic protein significantly enhanced COX2 promoter activity, but it requires the long DNA stretch (Fig. 6B).

These findings demonstrate a link between BMP signaling pathway and COX2 transcriptional regulation. To evaluate a direct involvement of COX2 in the maintenance of mesenchymal phenotype, A17 cells were treated with Dorsomorphin either alone or in combination with PGE_2, a major product of COX2 enzymatic activity. PGE_2 counteracted the mesenchymal–epithelial switch induced by Dorsomorphin and the PGE_2 treated cells maintained their typical spindle-like shape (Fig. 6C). Overall, these results provide evidence for the mechanistic role of BMP4/COX-2 axis in the control of A17 cell phenotype and behavior.

4. Discussion

Breast cancer remains one of the major causes of morbidity and mortality in Western Countries, despite progress in both knowledge and treatment. A deeper understanding of the underlying biology of breast cancer is necessary for the identification of new molecular targets and development of novel targeted therapeutics.

Studies of neoplastic tissues have provided evidence of self-renewing, stem-like cells within tumors, which have been called cancer stem cells. Cancer stem cells constitute a small minority of neoplastic cells within a tumor and are defined operationally by their ability to seed new tumors. For this reason, they have also been termed “tumor-initiating cells” [26].

Here we demonstrate that autocrinally BMP activated Smad signaling promotes migration, invasion and tumorigenicity of A17 cells, which are a murine model of mammary cancer strongly related to human mesenchymal cancer stem cells and basal-like breast cancer [9,10,17]. These cells express cytokeratin 14 suggesting a myoepithelial origin, but not E-cadherin, indicating a partial transdifferentiation toward a mesenchymal phenotype [12]. In particular, A17 cells give rise to aggressive mesenchymal tumors when injected into syngeneic mice, share molecular signature with mesenchymal stem cells and are endowed with the self-renewal ability being able to readily form mammospheres in suspension culture. *In vitro* analysis using Dorsomorphin [20,21] revealed that suppression of BMP signaling reduced A17 cell proliferation as well as anchorage-independent growth. Of note, Dorsomorphin treatment led to a morphological transition of A17 cells, which lost their elongated mesenchymal phenotype to acquire a polygonal epithelial-like shape. These phenotypical changes were associated with a decreased expression of Vimentin, a drastical reduction of the EMT markers Snail and Slug and an up-regulation of the epithelial markers E-cadherin and Cytokeratine-18. Similar results were obtained by transfection of A17 cells with siRNA molecules targeting BMP4. These experimental evidences suggest a role of BMP signaling in the control of the EMT-like phenotype of breast cancer cells. The EMT is presently recognized as a key process for tumor invasion and metastasis [23]. The hallmarks defining the EMT process are

Fig. 4. BMP signaling promotes migration, invasion and tumorigenicity of A17 cells. (A) Migration and (B) Matrigel invasion assays using the Boyden chamber model revealed a significant reduction in the migratory and invasive potentials of A17 cells upon treatment with the indicated concentrations of Dorsomorphin for 16 h. Cells were starved for 24 h before seeding them in Boyden chambers placed in 24 well plates containing either starvation media alone (negative control) or supplemented with 20% FBS (positive control) or 20 ng/ml BMP4, used as chemoattractants. Data are expressed as means ± SEM (left panels). ***P ≤ 0.001 One way ANOVA followed by Bonferroni's multiple comparison test. Representative images of migrating/invading cells treated as indicated (right panels). Magnification ×10. (C) Representative images of wounds at 0 and 16 h in the presence or absence of Dorsomorphin or BMP4. Confluent monolayers of A17 cells were scraped by a pipette tip to generate wounds and then were treated with vehicle or Dorsomorphin (0.5 μM or 2 μM) or BMP4 (20 ng/ml). The experiment was repeated twice obtaining comparable results. Magnification ×10. (D) Soft agar assay showing the impaired anchorage-independent growth of A17 cells treated with Dorsomorphin. Cells were plated in soft agar and left untreated or treated as indicated for two weeks. Representative images of the colonies are shown (left panels). Magnification ×10. The bars (right panels) represent the average number of colonies ± SEM (bottom) and the average diameter of foci ± SEM (top), after seven and 14 days. ***P ≤ 0.001 One way ANOVA followed by Bonferroni's multiple comparison test.

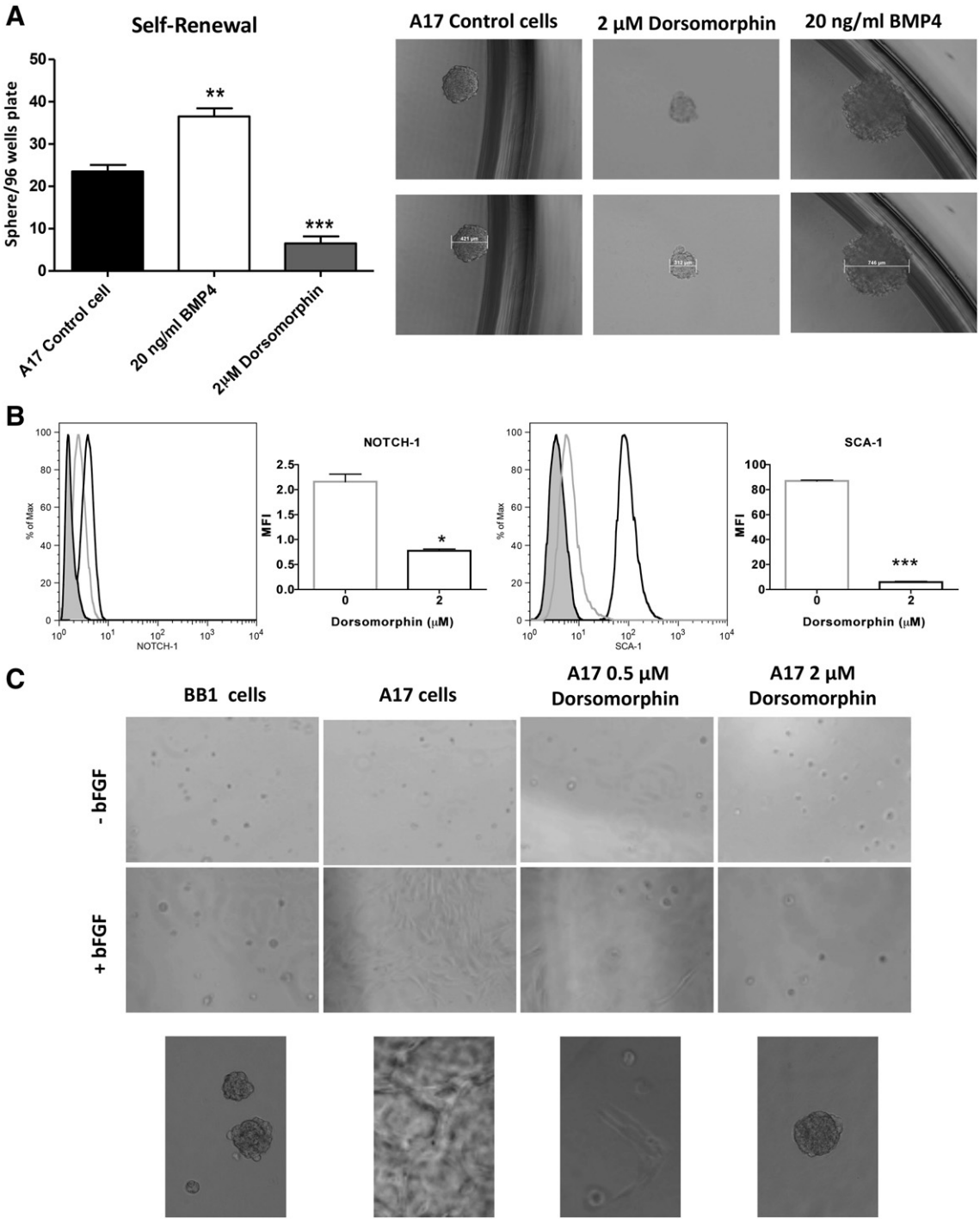

Fig. 5. Dorsomorphin causes loss of stem-like traits in A17 cells. (A) A17 cells form mammospheres in low attachment culture, as described in Materials and methods. Dorsomorphin impairs A17s self-renewal decreasing the number and the size of primary mammospheres, whereas BMP4 improves it. Quantification of mammosphere numbers for A17 cells. Error bars, mean ± SEM of triplicate experiments (left panel). Representative images of mammospheres formed by A17 cells (right panels). Magnification ×10. $^{**}P \leq 0.01$; $^{***}P \leq 0.001$ One way ANOVA followed by Bonferroni's multiple comparison test. (B) Representative flow cytometry histograms of SCA-1 and Notch-1 expression in control (vehicle alone) and Dorsomorphin treated A17 cells. Results were also shown as MFI (mean fluorescence intensity). $^{*}P \leq 0.05$; $^{***}P \leq 0.001$ One way ANOVA followed by Bonferroni's multiple comparison test. (C). Representative images of A17 and BB1 cells cultured in 3D culture (3D) on Matrigel supplemented or not with 20 μg/ml bFGF. Dorsomorphin inhibits formation of 3D tube-like structures by A17 cells. Magnification ×10. Detailed pictures were captured at 40× magnification.

the loss of E-cadherin mediated cell–cell adhesion and epithelial cell polarity concomitant to the acquisition of mesenchymal markers and increased motility and invasiveness [22]. Consistently, an autocrine BMP4 signaling pathway producing morphological alterations has been described in primary human normal ovarian surface epithelial (OSE) and epithelial ovarian cancer (OvCa) cells [27]. BMP4 induced EMT in primary OvCa cells through distinct mechanisms including the re-organization of actin fibers, up-regulation of Snail and Slug and down-regulation of E-cadherin. BMP4-stimulated OSE and ovarian cancer cell lines increased the expression of distinct target genes, including members of the ID gene family, ID1 and ID3, with a more pronounced response in OvCa compared with OSE cells [27]. Strikingly, BMP4 treatment enhanced cell mobility and invasion in OvCa cells but not in normal OSE [27]. These data suggest a key role of BMP4 at the crossroad between stemness and cancer.

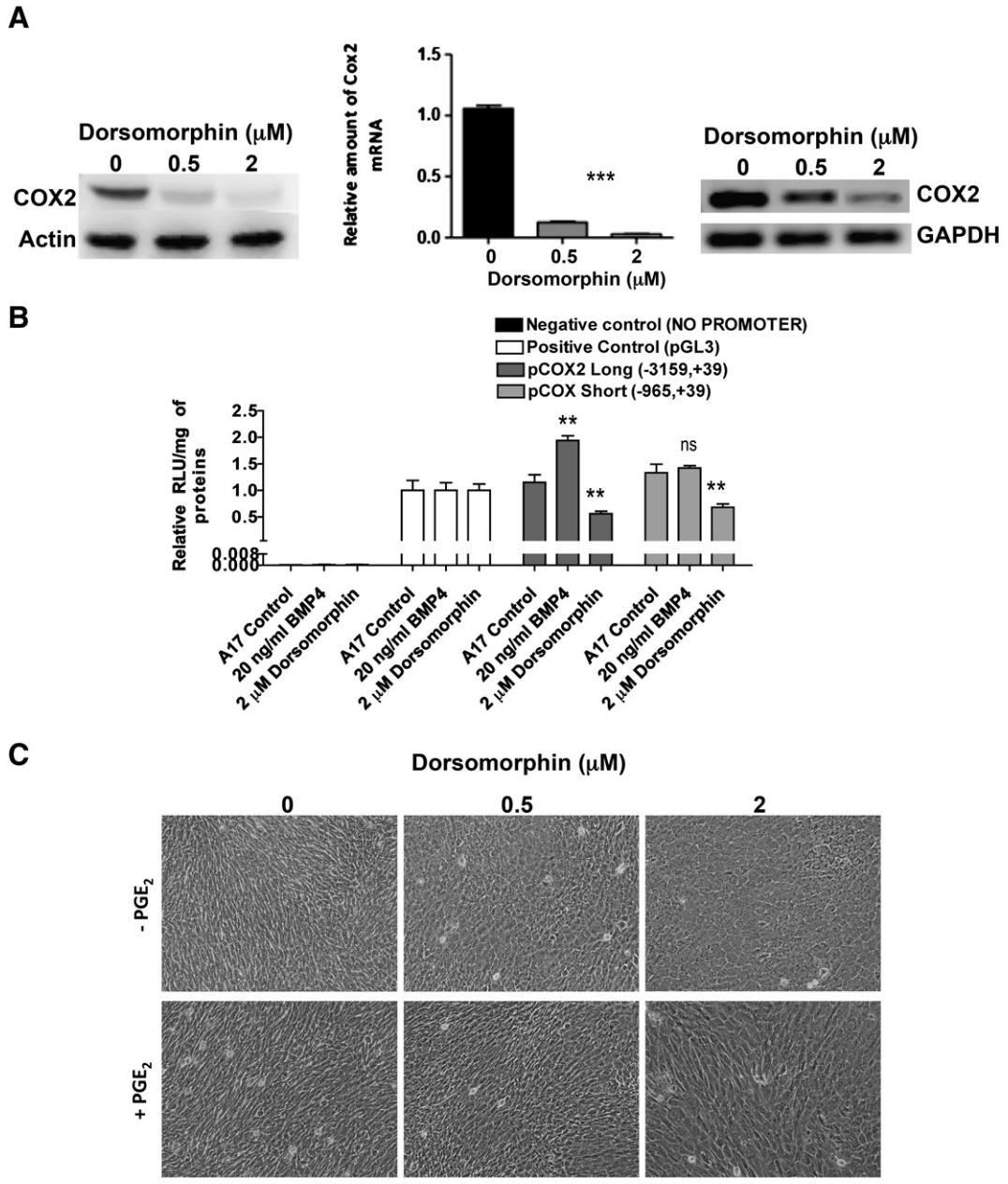

Fig. 6. BMP-dependent COX2 transcriptional expression sustains mesenchymal features of A17 cells. (A) Dorsomorphin inhibits COX2 expression in A17 cells. COX2 levels were evaluated in A17 cells treated with vehicle or Dorsomorphin (0.5 μM or 2 μM) for 96 h. COX2 protein levels were analyzed by Western blot in A17 cell extracts. Actin was used as loading control (left panel). COX2 mRNA levels were analyzed by RT-PCR (right panel) and were measured by quantitative RT-PCR, normalized to GAPDH, and shown as means ± SEM of three independent experiments (central panel). ***$P \leq 0.001$ One way ANOVA followed by Bonferroni's multiple comparison test. (B) Luciferase activity assay in A17 control cells, transfected with pGL3 vectors carrying luciferase reporter gene downstream of a short (−965, +39) or long (−3195, +39) stretch of COX2 promoter and then treated with 2 μM Dorsomorphin or 20 ng/ml BMP4. Negative control: pGL3 vector lacking promoter. Positive control: pGL3 vector, in which the luciferase expression is driven by SV40 promoter. The experiment was performed in quadruplicate; **$P \leq 0.01$ One way ANOVA followed by Bonferroni's multiple comparison test. (C) Representative images of A17 cells treated with vehicle or Dorsomorphin (0.5 μM or 2 μM), alone (upper panels) or in combination with 5 μM PGE_2 (lower panels) for 96 h. Cells were visualized by phase-contrast microscopy. Magnification ×10.

Accordingly, we have shown that BMP4 was expressed two-fold higher in A17 cells in comparison with normal stem cells [9]. In addition, A17 cell motility, invasiveness and adherence-independent growth were enhanced by BMP4 treatment. The reported results are in agreement with previous findings providing evidence that BMP signaling is hyperactivated in human and mouse breast tumors relative to normal tissue controls, and that it is highest in the basal breast cancer subtype [28]. Furthermore, numerous reports demonstrate a role for BMP signaling in promoting tumor cell migration and invasion [28–33], suggesting that BMP signaling pathway is essential in the control of breast cancer cell plasticity and may be targeted for therapeutic benefit.

Importantly, the EMT has recently been associated to stem cell phenotype [34]. EMT enables cancer cells to migrate from the primary tumor and colonize distant sites [34,35]. Accordingly, Dorsomorphin had a dramatic effect on A17 self-renewal and mammosphere formation and markedly reduced their expression of stem markers, whereas BMP4 stimulation increased the number and the size of primary mammospheres. These results indicate that BMP signaling confers plasticity and supports the cancer stem cell state, as already proposed by Balboni et al. [28]. In addition, a link between BMP signaling and COX2 transcriptional regulation was found implying a direct involvement of COX2 in the maintenance of mesenchymal phenotype of cancer stem-like cells. This new role of COX2

has been also proposed by Bisaro et al., who recently reported that COX2 sustains the mesenchymal features of breast cancer cells [17].

5. Conclusions

Taken together, studies presented here revealed the crucial role of BMP autocrine signaling in the maintenance of the mesenchymal stem cell phenotype, identifying potential target molecules for therapies aimed to reduce recurrence risk. Indeed, cancer stem cells present in breast tumors while being intrinsically resistant to conventional therapies, have the ability to self renew and cause tumor recurrence. The residual tumors after therapy, with dramatic enrichment of the cancer stem cells, have all the hallmarks of EMT [36]. The conversion of mesenchymal stem cells to epithelial cells by blocking BMP pathway could represent a strategy to interfere with recurrences and metastatization in breast cancer.

Supplementary data to this article can be found online at http://dx.doi.org/10.1016/j.cellsig.2013.11.022.

Conflict of interest statement

None declared.

Acknowledgments

We thank Prof. Paola Defilippi for fruitful discussions and suggestions.

This work was supported by the Italian Association for Cancer Research [IG11889 to A.A.]; and the Italian Ministry for the Universities and Research [2008W3KW2A_002 to A.A.].

References

[1] K. Miyazono, et al., J. Biochem. 147 (2010) 35–51.
[2] K. Miyazono, et al., Cytokine Growth Factor Rev. 16 (2005) 251–263.
[3] R. Derynck, et al., Nature 425 (2003) 577–584.
[4] C.H. Heldin, et al., Nature 390 (1997) 465–471.
[5] J.P. Thawani, et al., Neurosurgery 66 (2010) 233–246.
[6] J.M. Ketolainen, et al., Breast Cancer Res. Treat. 124 (2010) 377–386.
[7] A.C. Varga, et al., Oncogene 24 (2005) 5713–5721.
[8] J.A. Dutko, et al., Cell 145 (2011) 636.
[9] M. Galiè, et al., Oncogene 27 (2008) 2542–2551.
[10] C. Marchini, et al., PLoS One 5 (2010) e14131.
[11] G. Singh-Ranger, et al., Breast Cancer Res. Treat. 109 (2008) 189–198.
[12] M. Galiè, et al., Carcinogenesis 26 (2005) 1868–1878.
[13] M. Galie, et al., Neoplasia 7 (2005) 528–536.
[14] J. Zalvide, et al., Mol. Cell. Biol. 15 (1995) 5800–5810.
[15] G. Dontu, et al., Genes Dev. 17 (2003) 1253–1270.
[16] J. Debnath, et al., Methods 30 (2003) 256–268.
[17] B. Bisaro, et al., Breast Cancer Res. 14 (2012) 137–148.
[18] Y. Yokota, et al., J. Cell. Physiol. 190 (2002) 21–28.
[19] O. Korchynskyi, P. ten Dijke, J. Biol. Chem. 277 (2002) 4883–4891.
[20] C.C. Hong, et al., Cytokine Growth Factor Rev. 20 (2009) 409–418.
[21] P.B. Yu, et al., Nat. Chem. Biol. 4 (2008) 33–41.
[22] R. Kalluri, et al., J. Clin. Invest. 119 (2009) 1420–1428.
[23] K. Polyak, et al., Nat. Rev. Cancer 9 (2009) 265–273.
[24] D. Ponti, et al., Cancer Res. 65 (2005) 5506–5511.
[25] A.R. Susperregui, et al., Mol. Endocrinol. 25 (2011) 1006–1017.
[26] T. Reya, et al., Nature 414 (2001) 105–111.
[27] B.L. Thériault, et al., Carcinogenesis 28 (2007) 1153–1162.
[28] A.L. Balboni, et al., Cancer Res. 73 (2013) 1020–1030.
[29] D. Guo, et al., Mol. Cell. Biochem. 363 (2012) 179–190.
[30] C.Y. Chiu, et al., Mol. Cancer Res. 10 (2012) 415–427.
[31] J.H. Clement, et al., Int. J. Oncol. 27 (2005) 401–407.
[32] U. Maegdefrau, et al., Exp. Mol. Pathol. 92 (2012) 74–81.
[33] Y. Katsuno, et al., Oncogene 27 (2008) 6322–6333.
[34] S.A. Mani, et al., Cell 133 (2008) 704–715.
[35] J.M. Bailey, et al., J. Cell. Biochem. 102 (2007) 829–839.
[36] B. Dave, et al., Breast Cancer Res. 14 (2012) 202–206.